Supporting Information

Mechanism of *in-situ* confining carbon dots in phthalamide crystal for room-temperature phosphorescence

Xingmei Li,[1&] Haixin Kang,[2&] Yingying Zhao,[1] Tong Chen,[1] Jingxia Zheng,[1,3*] Lin Chen,[1,3] Bin Liu,[4] Yongzhen Yang,[1,3*] Xuguang Liu[2*]

[1] Key Laboratory of Interface Science and Engineering in Advanced Materials, Ministry of Education, Taiyuan University of Technology, Taiyuan 030024, China

[2] College of Materials Science and Engineering, Taiyuan University of Technology, Taiyuan 030024, China

[3] Shanxi-Zheda Institute of Advanced Materials and Chemical Engineering, Taiyuan 030000, Shanxi, China;

[4] School of Energy and Power Engineering, North University of China, Taiyuan 030051, China

& These authors contributed equally to this work and should be considered co-first authors.

*Corresponding author: E-mail: zhengjingxia@tyut.edu.cn;
yangyongzhen@tyut.edu.cn;
liuxuguang@tyut.edu.cn

Table S1 Raw materials and dosages

Product	Raw material (dosage)
CDs-a	Phthalamide (1.6 g) and ethylene glycol (20 mL)
CDs-b	Phthalamide (1.6 g), ethylene glycol (10 mL), and formamide (10 mL)
CDs-c	Phthalimide (1.6 g) and ethylene glycol (20 mL)
CDs-d	Phthalimide (1.6 g), ethylene glycol (10 mL), and formamide (10 mL)

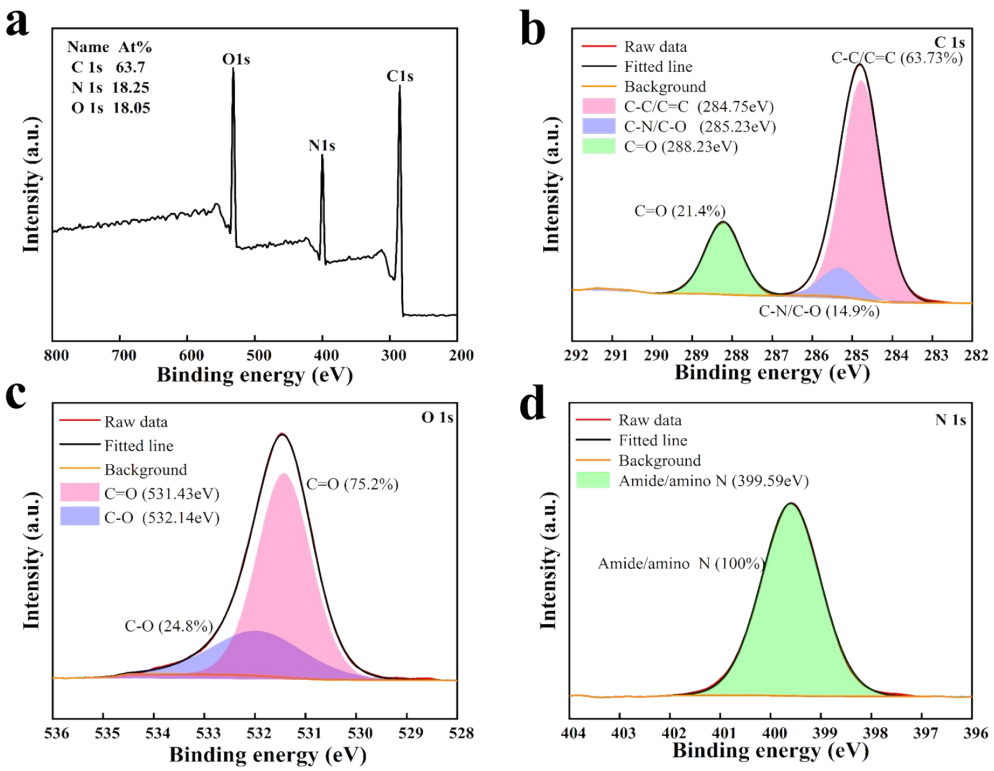

Figure S1 (a) XPS full scan spectrum of CDs@phthalamide; High-resolution (b) C 1s, (c) O 1s, and (d) N1s XPS spectrum of CDs@phthalamide

Table S2 RTP properties of different CDs-based composites

Product	Raw material	RTP
CDs-A	Phthalic acid and ethylene glycol	×
CDs-B	Phthalic acid and formamide	×
CDs-C	Formamide and ethylene glycol	×
CDs-D	Formamide	×
CDs-E	Ethylene glycol	×
CDs@phthalamide	Phthalamide, ethylene glycol, and formamide	√

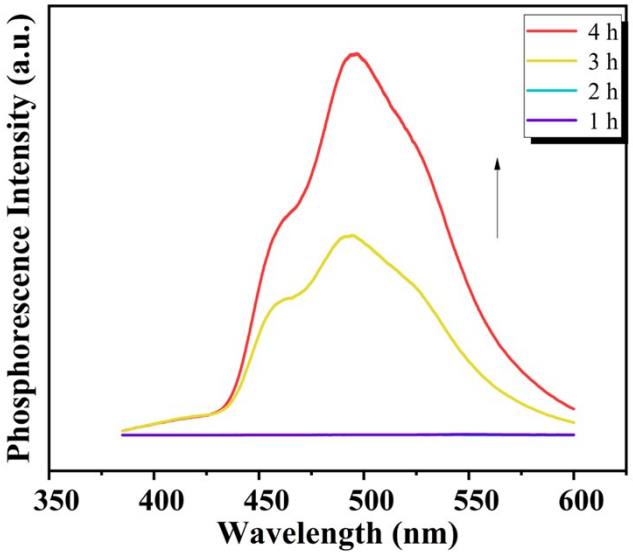

Figure S2 RTP emission spectra of the products obtained at different reaction times (λ_{ex}=365 nm)

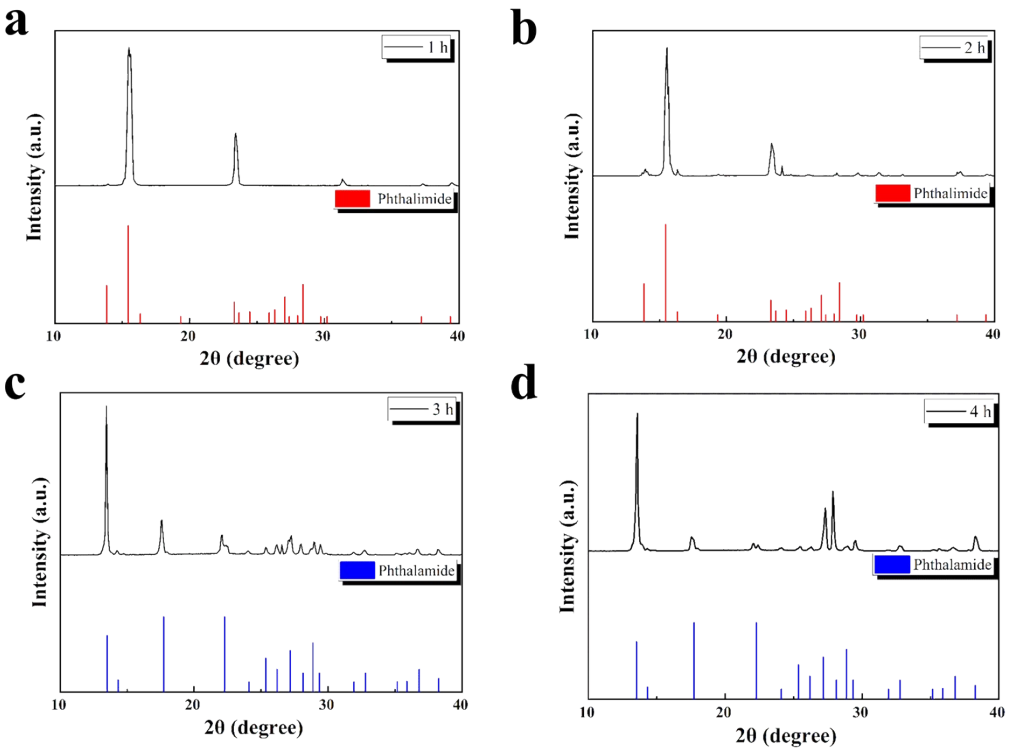

Figure S3 XRD patterns of the products obtained at different reaction times

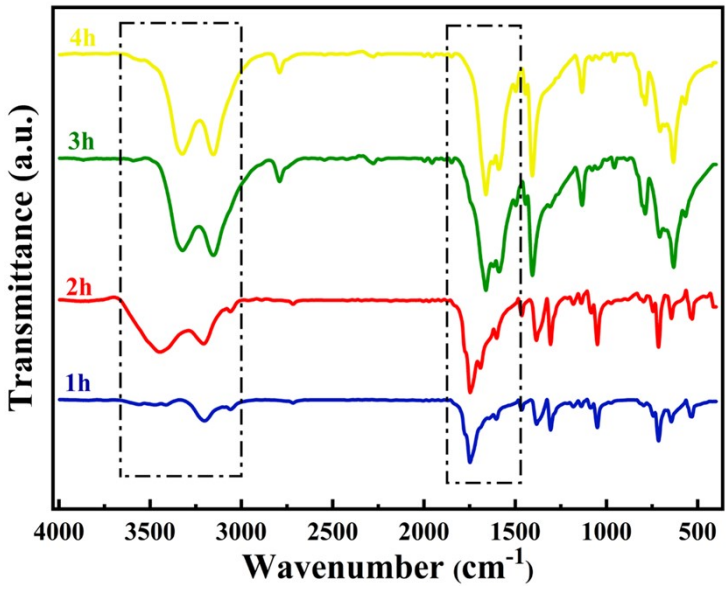

Figure S4 FTIR spectra of the products obtained at different reaction times

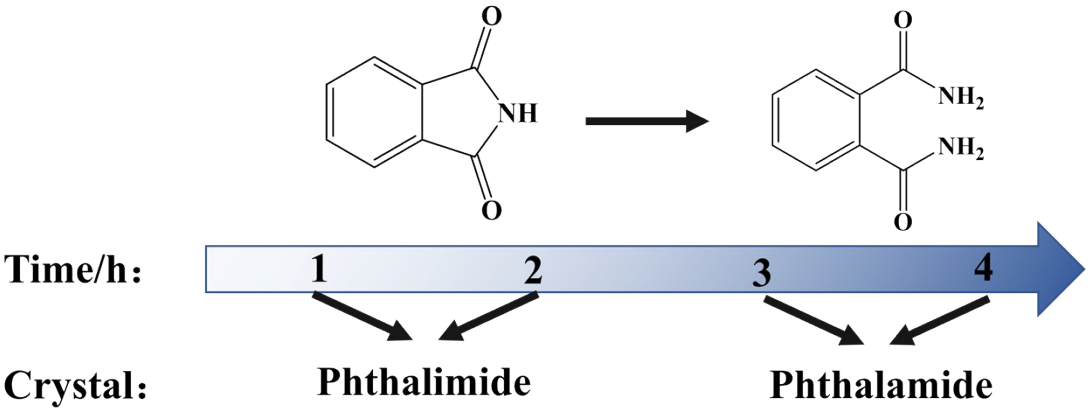

Figure S5 Schematic of the products obtained at different reaction times

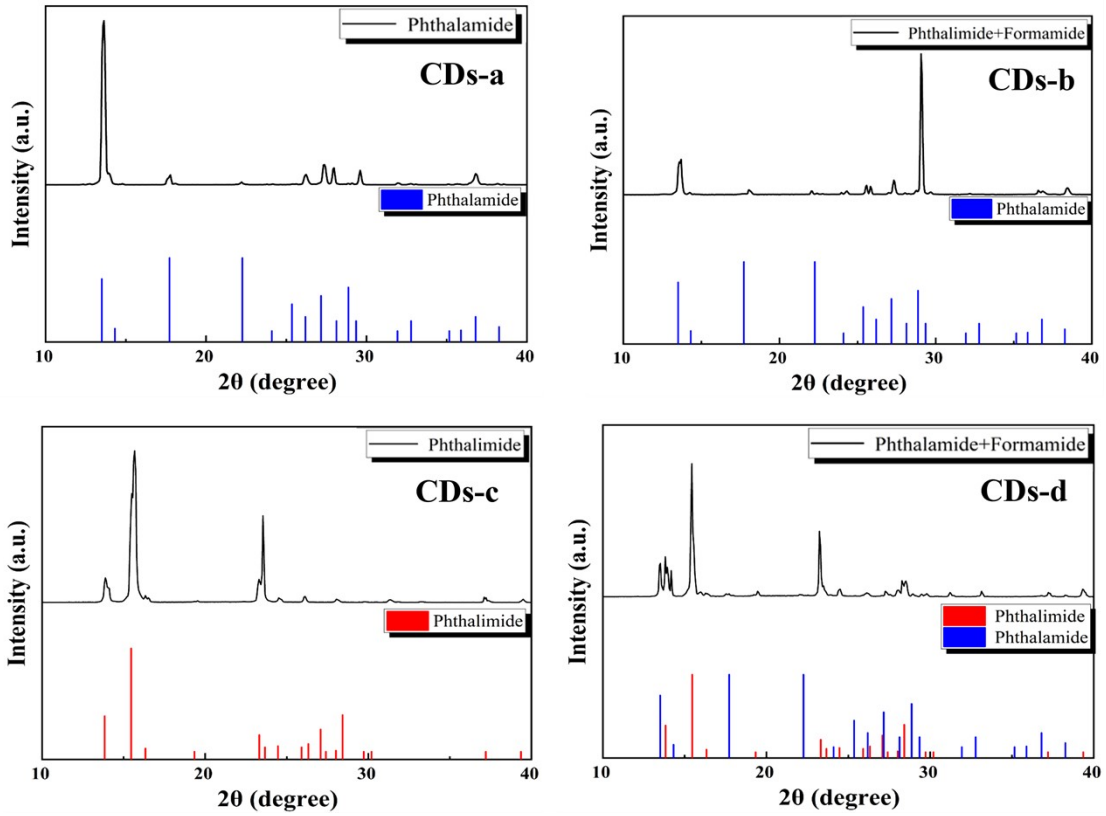

Figure S6 XRD patterns of the products obtained with different raw materials

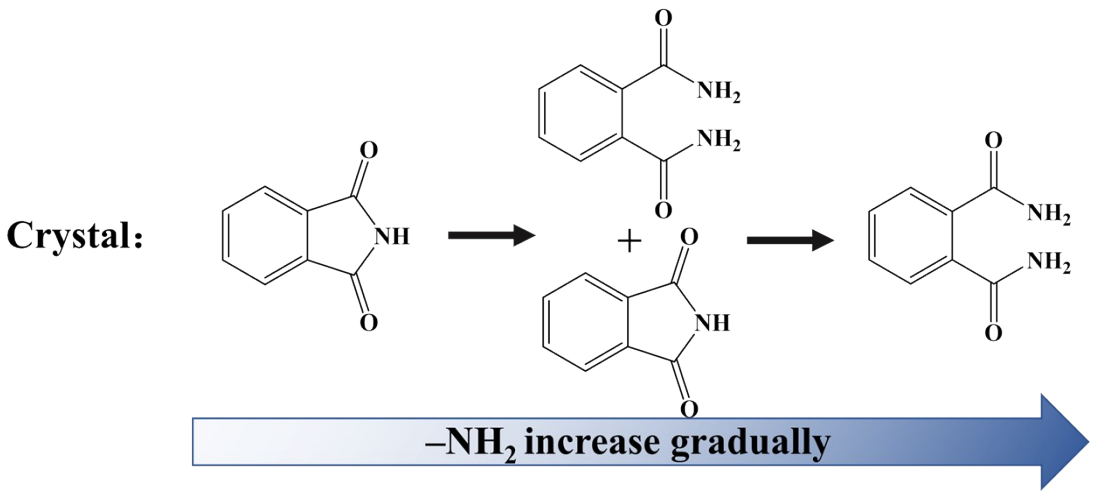

Figure S7 Schematic of organic crystal transition in products obtained from different reaction materials

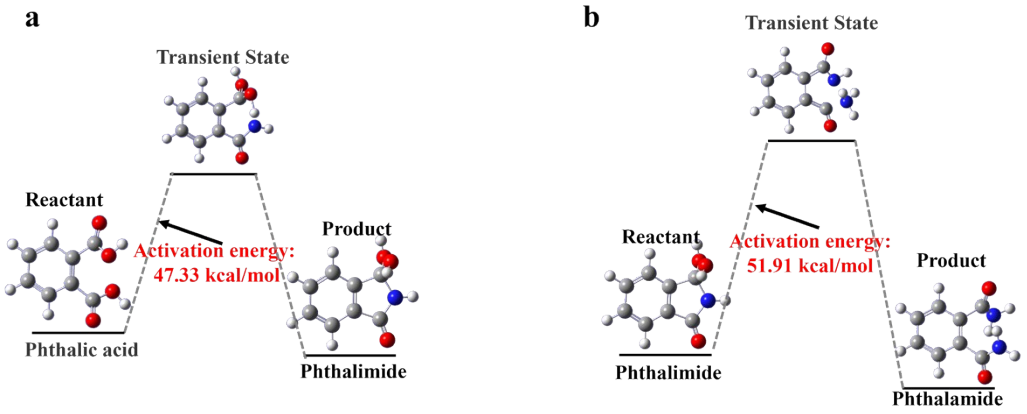

Figure S8 Schematic of activation energy of (a) phthalimide and (b) phthalamide in vacuum

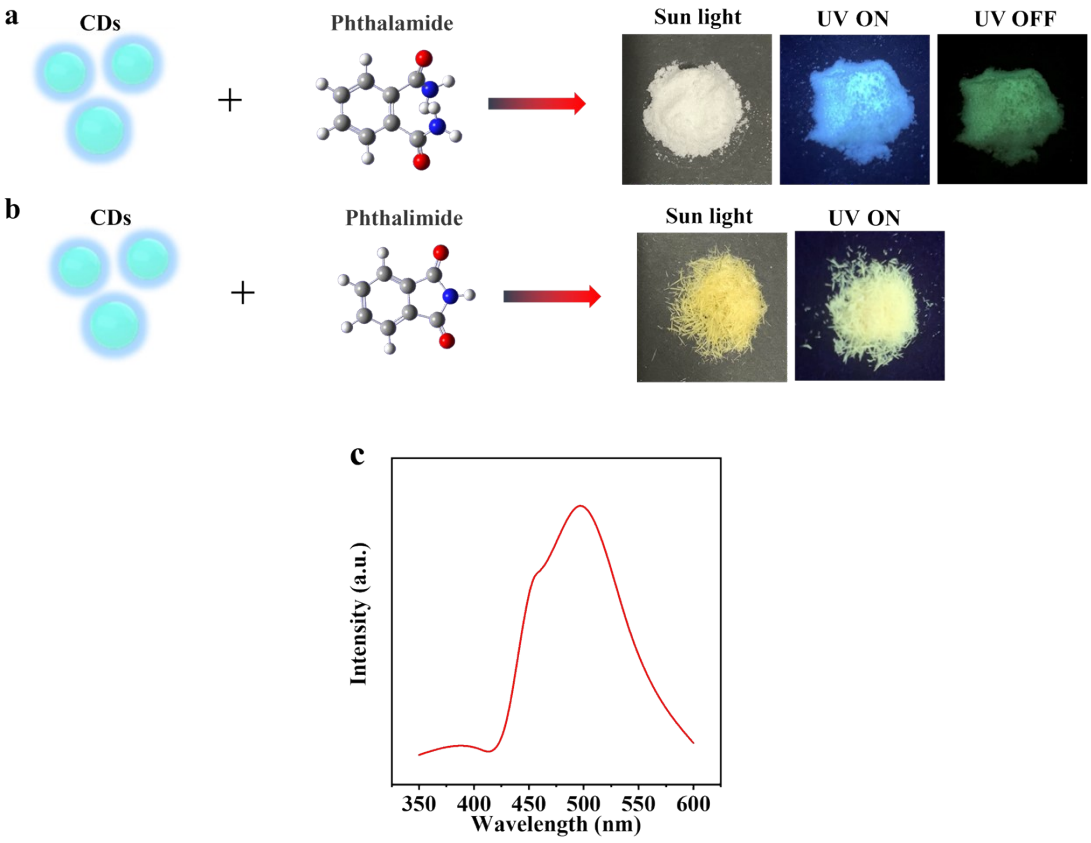

Figure S9 Photos of R-CDs@phthalamide and R-CDs@phthalimide powder under sunlight, UV lamp (λ_{ex}=365 nm), and after UV lamp turning off; (c) RTP emission spectrum of R-CDs@phthalamide

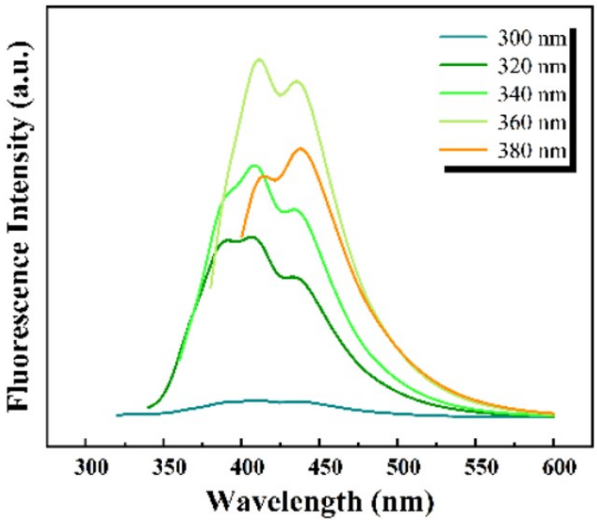

Figure S10 FL emission spectra of CDs at different excitation wavelengths

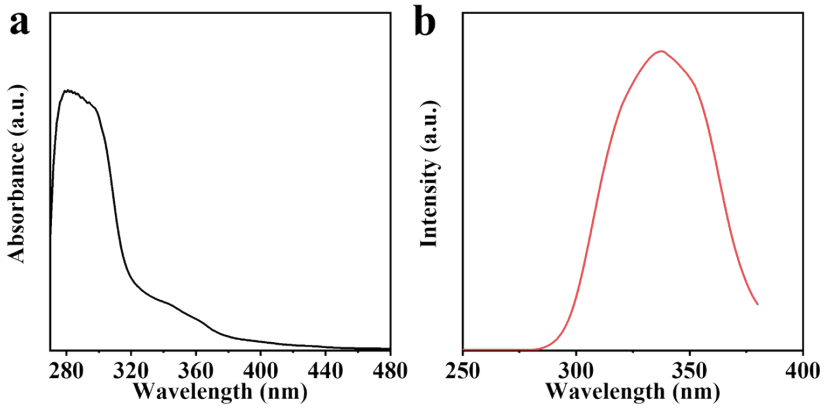

Figure S11 (a) UV-vis spectra and (b) excitation spectra of CDs

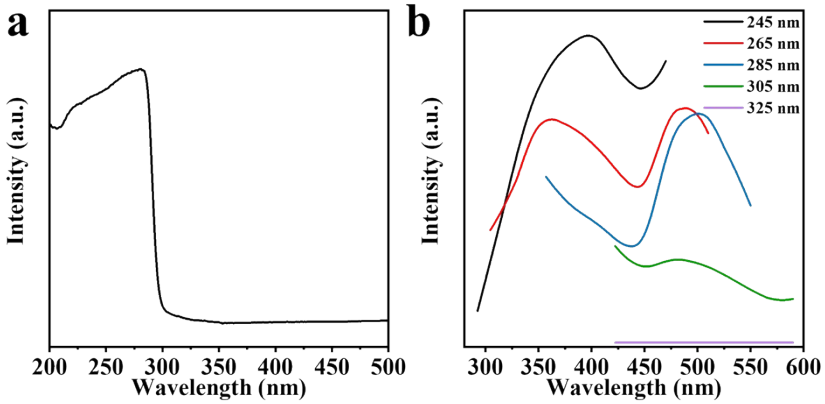

Figure S12 (a) Excitation spectra and (b) FL emission spectra of phthalimide

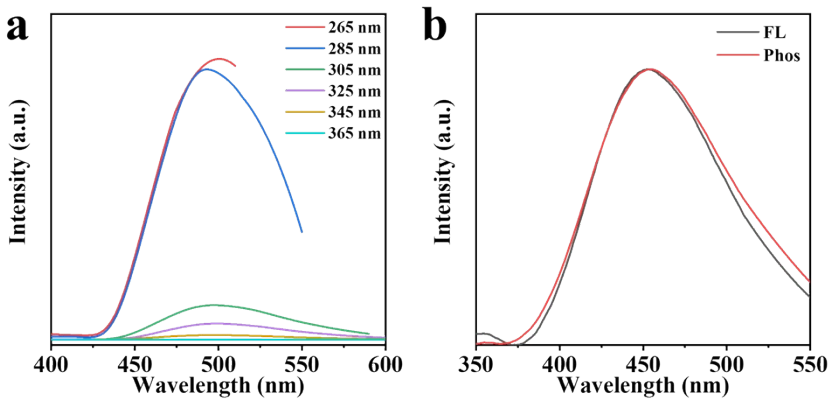

Figure S13 (a) RTP emission spectra of phthalamide and (b) FL and RTP emission spectra at low temperature of 77 K (λ_{ex} = 285 nm)

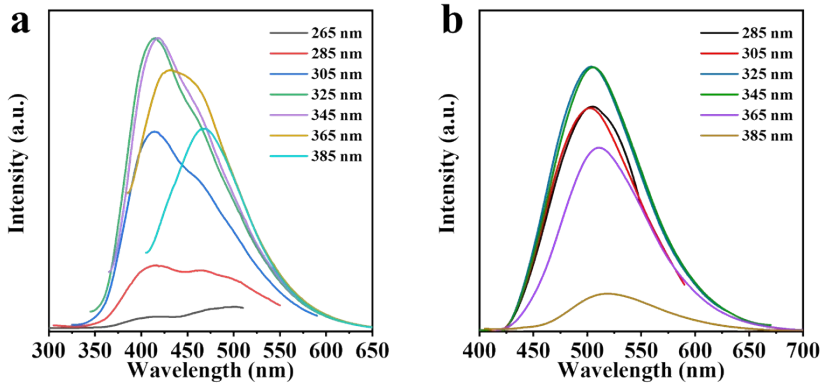

Figure S14 (a) FL emission and (b) RTP emission spectra of CDs@phthalamide under different excitation wavelengths

Table S3 Summary of the afterglow lifetimes of CDs@phthalamide

Sample	τ_1 (ms)	Proportion (%)	τ_2 (ms)	Proportion (%)	τ_3 (ms)	Proportion (%)
CDs@phthalamide	17.31	5.89	232.72	47.65	708.16	46.47

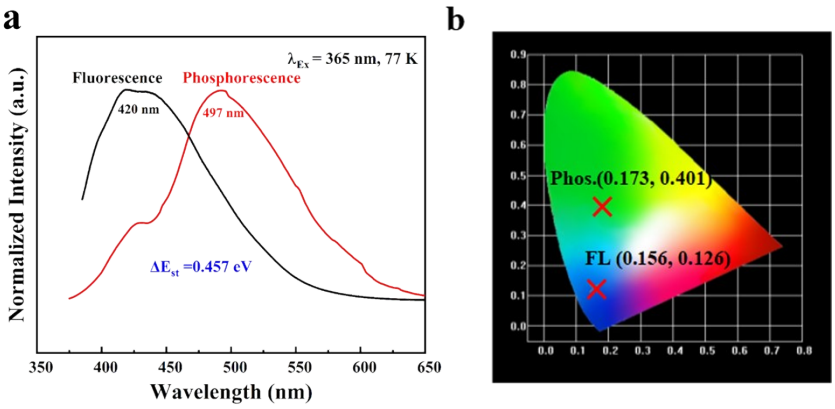

Figure S15 (a) FL and RTP emission spectra (77 K, λ_{ex}=365 nm) and (b) CIE coordinates of FL and RTP of CDs@phthalamide powder

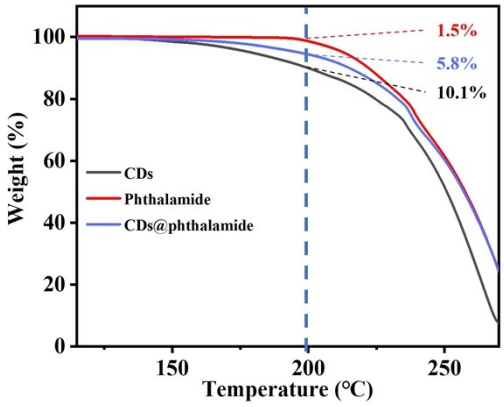

Figure S16 TG curves of CDs, phthalamide, and CDs@phthalamide composite (N_2 atmosphere, 10 °C/min)

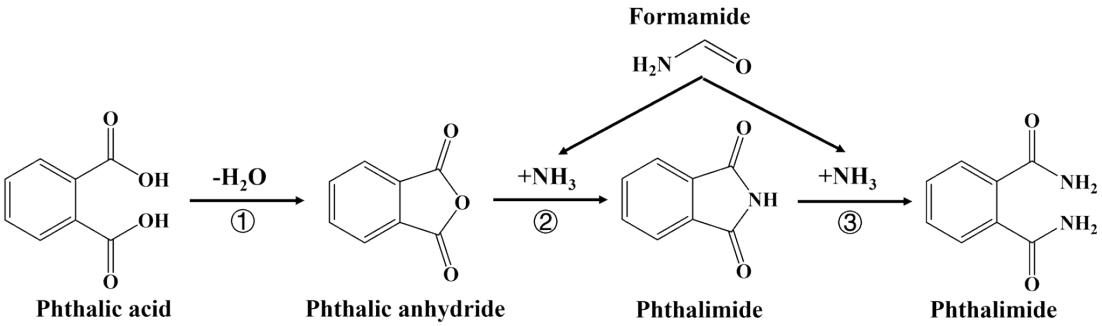

Figure S17 Formation process of CDs@phthalamide

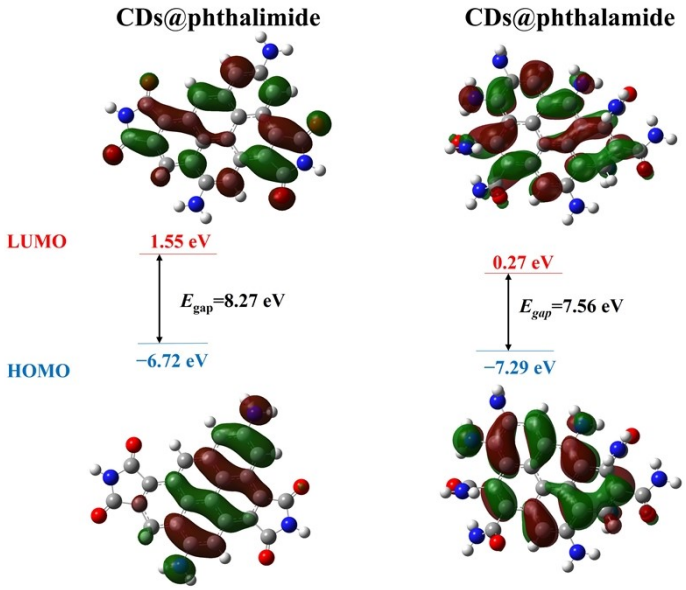

Figure S18 The HOMO-LUMO electron cloud distribution and energy levels theoretical calculations of CDs@phthalimide and CDs@phthalamide structural models

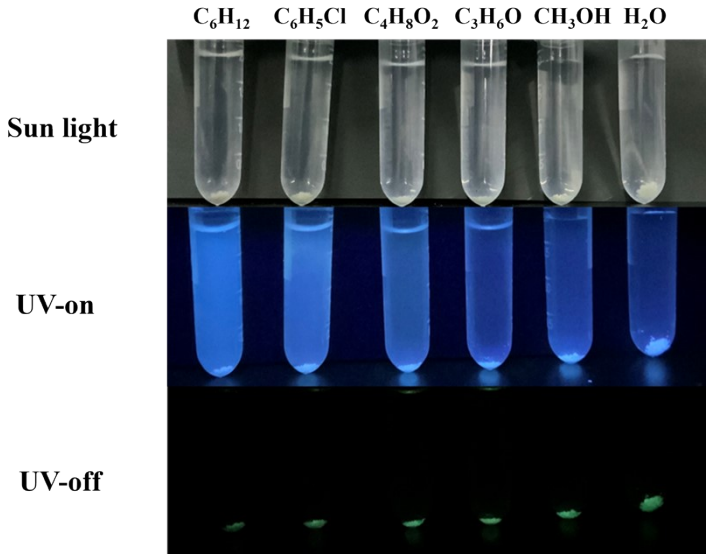

Figure S19 Photographs of CDs@phthalamide powder in different polarity solvents (sunlight, UV on, and UV off)

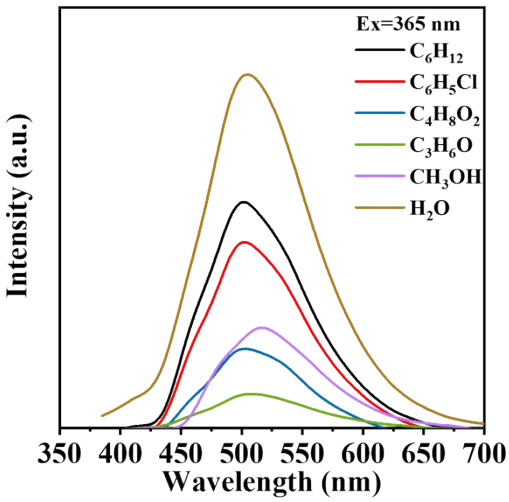

Figure S20 RTP emission spectra of CDs@phthalamide powder in different polarity solution (λ_{ex}=365 nm)

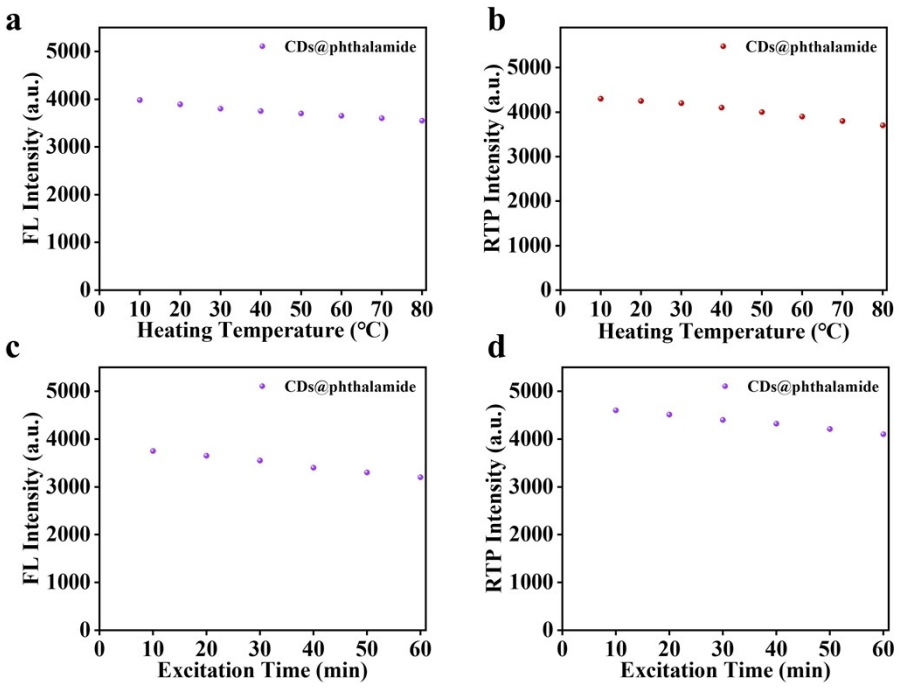

Figure S21 (a) The fluorescence and (b) RTP intensities of CDs@phthalamide after 15-minute heat treatment at different temperatures; (c) The fluorescence and (d) RTP intensities of CDs@phthalamide under continuous excitation for 10–60 minutes

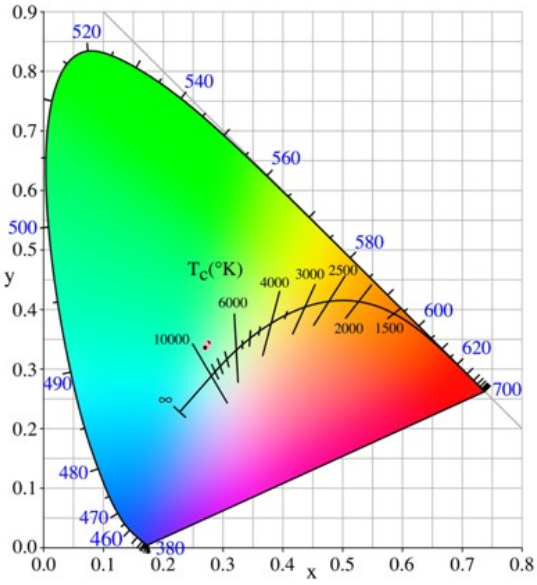

Figure S22 CIE coordinates of the time-delayed WLED measured at different voltages

Table S4 Comparison of the properties of different RTP materials

Samples	Matrix	RTP lifetime (ms)	RTP QY	Stability	References
u-CDs@NaOH	NaOH	257.12	4.33%	-	[1]
uCDs@150	Urea	281	-	-	[2]
PCDs	BA	293	5.15%	-	[3]
CDs-LDHs	LDH	170.95	1.48%	-	[4]
CDs-LDHs@PVA	PVA	412.53	3.13%		
CD–APS1	$KAl(SO_4)_2 \cdot x(H_2O)$	707	-	-	[5]
CDs-1	PVA	103	5.3%	★	[6]
M-CDs	Melamine	664	25%	-	[7]
PACD/polymer	Polymer	652		-	[8]
AM-CDs	AM	697.58	17.3%	-	[9]
CD-5.6	Urea	419	PLQY26%	■	[10]
rCDs	Urea	211	PLQY30%	▲	[11]
CDs@phthalamide	Phthalamide	441	PLQY26% RTP QY10.1%	●	This work

★No significant photoluminescence (PL) intensity degradation was observed after 6 months of storage at room temperature.

■Only a slight (<4%) decrease in the initial PL intensity was observed under continuous UV illumination (1 W) for 10 hours.

▲ Repeatable 30-minute excitation cycles showed no significant degradation. Thermal treatment at 373 K for 2 hours retained over 90% of the initial PL intensity. The afterglow intensity in aqueous media was more than twice that of the dry powder.

●The fluorescence and RTP intensities showed less than 12% decrease after 15-minute heat treatment across the temperature range of 10–60 °C. Following continuous excitation for 10–60 minutes, the fluorescence and RTP intensities exhibited less than 10% reduction.

References:

[1] C. Li, X. Zhao, C. Li, J. Hu, J. Zhu, Q. Lou, N. Chen, Z. Song, X. Chen, G. Pan, Efficient color-tunable room temperature phosphorescence through confining carbon dots in ionic crystal, J. Alloys and Compd., 2023, 948, 169674.

[2] L. Chen, S. Zhao, Y. Wang, S. Yu, Y. Yang, X. Liu, Long-lived room-temperature phosphorescent complex of B, N, P co-doped carbon dots and silica for afterglow imaging, Sensor. Actuat. B-Chem., 2023, 390, 133946.

[3] M. Cheng, L. Cao, H. Guo, W. Dong, L. Li, Green synthesis of phosphorescent carbon dots for anticounterfeiting and information encryption, Sensors-Basel, 2022, 22, 2944.

[4] R. Wang, Y. Zhu, Z. Xia, K. Liang, L. Kong, J. Liu, W. Shi, C. Lu, Room temperature phosphorescence of carbon dots activated by layered double hydroxides for application in information encryption, J. Mater. Chem. C, 2022, 10, 17182–17189.

[5] X. Dong, L. Wei, Y. Su, Z. Li, H. Geng, C. Yang, Y. Zhang, Efficient long lifetime room temperature phosphorescence of carbon dots in a potash alum matrix, J. Mater. Chem. C, 2015, 3, 2798–2801.

[6] F. Zhao, T. Zhang, Q. Liu, C. Lü, Aphen-derived N-doped white-emitting carbon dots with room temperature phosphorescence for versatile applications, Sensor. Actuat. B-Chem., 2020, 304, 127344.

[7] Y. Gao, H. Zhang, Y. Jiao, W. Lu, Y. Liu, H. Han, X. Gong, S. Shuang, C. Dong, Strategy for activating room-temperature phosphorescence of carbon dots in aqueous environments, Chem. Mater., 2019, 31, 7979–7986.

[8] H. Gou, Y. Liu, G. Zhang, Q. Liao, X. Huang, F. Ning, C. Ke, Z. Meng, K. Xi, Lifetime-tunable room-temperature phosphorescence of polyaniline carbon dots in adjustable polymer matrices, Nanoscale, 2019, 11, 18311–18319.

[9] Z. Li, Y. Wu, X. Luo, X. Dong, K. Pan, F. Xiu, J. Liu, Stabilizing carbon dot phosphorescence

in aqueous solutions by hydrogen-bonded networks for dual-wavelength-driven information encryption, ACS Appl. Nano Mater., 2023, 6, 20251–20257.

[10] J. Zhu, X. Bai, X. Chen, H. Shao, Y. Zhai, G. Pan, H. Zhang, E. Ushakova, Y. Zhang, H. Song, A. Rogach, Spectrally tunable solid state fluorescence and room-temperature phosphorescence of carbon dots synthesized via seeded growth method, Adv. Opt. Mater., 2019, 7, 1801599.

[11] J. Tan, Z. Yi, Y. Ye, X. Ren, Q. Li, Achieving red room temperature afterglow carbon dots in composite matrices through chromophore conjugation degree controlling, J. Lumin., 2020, 223, 117267.

Table S5 Comparison table of time-delay WLED application performance

Afterglow time(s)	CIE	CCT (K)	CRI	References
2	(0.33, 0.32)	5599	90.04	[1]
2	(0.396, 0.409)	3791	-	[2]
-	(0.32, 0.34)	6202	81.1	[3]
3	(0.27, 0.33)	8832	84	This work

References:

[1] X. Bao, K. Zhao, Z. Tian, W. Sun, H. Wang, Z. Liu, L. Zhao, H. Li, X. Yuan, Blue light-excited carbon dot/C_3N_4 nanocomposites with long-lived thermally activated delay fluorescence for anti-counterfeiting and illumination, ACS Appl. Nano Mater., 2024, 7, 6681–6690.

[2] J. Zhu, J. Hu, Q. Hu, X. Zhang, Elena V. Ushakova, K. Liu, S. Wang, X. Chen, C. Shan, Andrey L. Rogach, X. Bai, White light afterglow in carbon dots achieved via synergy between the room-temperature phosphorescence and the delayed fluorescence, Small, 2022, 18, 2105415.

[3] W. Sun, Y. Zhang, G. Yin, S. Lu, Afterglow of dual-confined carbon dots ranging from blue to near-infrared, Adv. Funct. Mater., 2024, 34, 2402346.

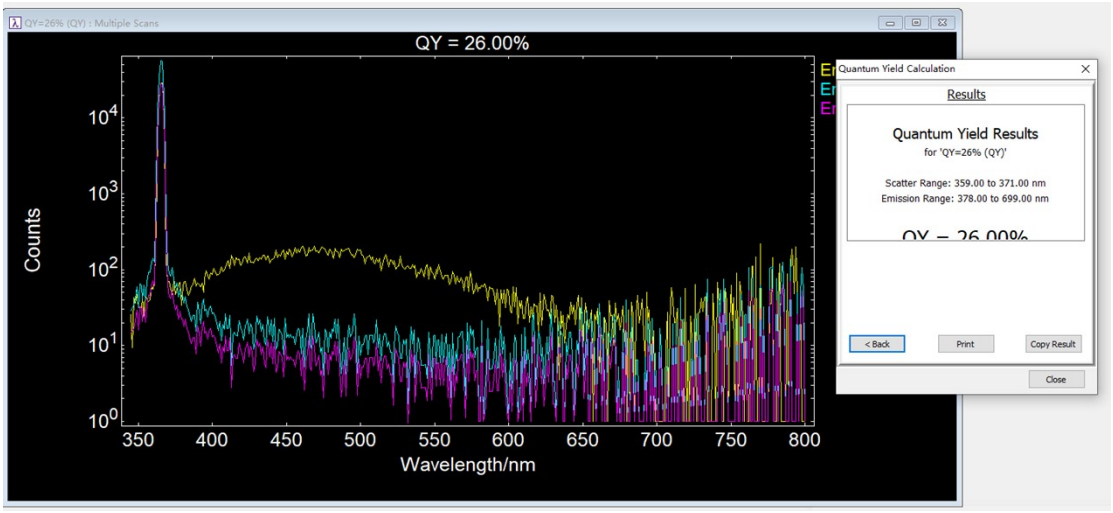

Figure S23 The absolute PLQY values of CDs@phthalamide

Calculation of RTP QY: First, the absolute photoluminescence quantum yield (PLQY) of CDs@phthalamide was measured at room temperature on an FLS1000 steady-state/transient fluorescence spectrometer from Edinburgh with an integrating sphere. Then, the ratio of the integrated area of RTP spectrum to the integrated area of the total PL spectrum was calculated, and finally the RTP QY was calculated according to the formula[1].

$$\emptyset_{RTP} = \frac{B}{A} \times \emptyset_{PL}$$

Where $\emptyset_{PL}$ represent the value of PLQY, and A and B represent the integrated area of the total photoluminescence spectrum and phosphorescence spectrum, respectively.

References:

[1] H. Shi, Y. Wu, J. Xu, C. Zhou, H. Xu, W. Ye, Y. Yin, Z. Wang, R. Su, Z. An, H. Shi, Enhancing blue phosphorescence in matrix-free carbon dots through covalent crosslinking. Chem. Eng. J. 476 (2023) 146524.